Helicene Bis(pyrazol-1-yl)pyridine Ligands for Luminescent Transition-Metal Complexes

Alexandre Abhervé, Kevin Martin, Andreas Hauser, Narcis Avarvari

Helicene bis(pyrazol-1-yl)pyridine ligands for luminescent transition metal complexes

Alexandre Abhervé,*[a] Kévin Martin,[a] Andreas Hauser,[b] and Narcis Avarvari*[a]

[a] Dr. A. Abhervé, Dr. K. Martin, Dr. N. Avarvari

MOLTECH-Anjou, UMR 6200, CNRS, UNIV Angers, 2 bd Lavoisier, 49045 ANGERS Cedex, France. E-mail: alexandre.abherve@univ-angers.fr; narcis.avarvari@univ-angers.fr

[b] Prof. A. Hauser

Department of Physical Chemistry, University of Geneva, 30 Quai Ernest-Ansermet, CH-1211 Geneva, Switzerland.

Supporting Information and ORCID(s) from the author(s) for this article are available on the WWW under http://doi.org/10.1002/ejic.000000000.

ORCID
Alexandre Abhervé: 0000-0002-3883-310X
Narcis Avarvari: 0000-0001-9970-4494

Abstract: We describe herein the synthesis of 2,6-bis(pyrazol-1-yl)pyridine (1-bpp) ligands substituted by helicene units in the 4-position of the pyridine ring. The two-step procedure afforded the molecules bpp[*n*]helicene (*n* = 4, 5 and 6) and methyl-bpp[4]helicene, abbreviated as **4**, **5**, **6** and **4m** respectively, with overall good yields. This series of ligands shows fluorescence in the violet region, with a red shift of the emission when increasing the number of aromatic rings in the helicene unit. The tridentate fluorophores have been reacted with $Re(CO)_5Cl$ and $[Ru(terpy)Cl_3]$ to prepare a series of transition metal complexes formulated as $[Re^{I}(\boldsymbol{n})(CO)_3Cl]$ (***n*** = **4** and **5**) and $[Ru^{II}(\boldsymbol{n})(terpy)](PF_6)_2$ (***n*** = **4**, **4m**, **5** and **6**). The compounds $[Re^{I}(\mathbf{4})(CO)_3Cl]\cdot(CH_2Cl_2)_{0.5}(H_2O)$ and $[Ru^{II}(\mathbf{4m})(terpy)](PF_6)_2$ crystallized in the centrosymmetric space groups $P2_1/n$ and P-1 respectively, and thus present both *M* and *P* helicene units in their crystal structures. The absorption and emission properties of the complexes have been studied. All complexes show luminescence at 77 K in frozen DCM solution. The tricarbonyl complex $[Re^{I}(\mathbf{5})(CO)_3Cl]$ shows a strong emission band with two peaks at 540 nm and 580 nm, which could be attributed to ligand-localized π-π* phosphorescence due to the extended π system of the ligand. The heteroleptic Ru(II) complexes show emission bands above 600 nm attributed to the terpyridine-based ^{3}MLCT state.

Introduction

Helicenes have recently attracted a lot of attention in the field of chiral materials.[1] Thanks to their helical π-conjugated backbone, they present exceptional chiroptical properties such as high optical activity, intense electronic circular dichroism (ECD) and circularly polarized luminescence (CPL).[2] Helicene-based transition metal complexes have been investigated in order to obtain innovative molecular devices which combine the chiroptical properties of the helicene unit with the properties of the metal center.[3] While azahelicene ligands and their Ag(I) complexes have been described by Starý et al. back in 2008,[4] more recent reports by

Crassous et al. deal with azahelicene appended pyridine ligands and complexes,[5] such as helicene-2,2'-bipyridine and its cycloplatinated complex. The latter shows electronic CD and CPL acid/base switching,[5a] while for a bis-helicenic terpyridine ligand Zn(II) coordination induced chiroptical modulation has been observed.[5b] Another interesting tridentate ligand closely related to terpyridine is 2,6-bis(pyrazol-1-yl)pyridine (1-bpp), which can be easily functionalized at its periphery with a variety of substituents,[6] thus providing the possibility to finely tune the properties of the derived complexes. Accordingly, Fe(II) complexes of 1-bpp usually present very abrupt spin transitions with thermal hysteresis close to room temperature,[7] and they often exhibit spin-crossover induced by irradiation (light-induced excited spin state trapping effect, LIESST) with relatively long lifetimes of the photoinduced metastable states.[7d] Likewise, 1-bpp derivatives and 1-bpp-based Re^{I} and Ru^{II} complexes have been investigated for their photophysical properties.[8,9] Chandrasekar et al. have described the violet fluorescence of a series of *back-to-back* coupled 1-bpp ligands,[10] and reported very recently the luminescence of the methylthiophenyl-substituted 1-bpp.[11] $Re(CO)_3X$ (X = Cl or Br) fragments have been combined with 1-bpp and a thiophene-functionalized 3-bpp to prepare the complexes of formula $[Re(1\text{-bpp})(CO)_3Cl]$ and $[Re(3\text{-bpp})(CO)_3Br]$ respectively,[8] while $[Ru(terpy)Cl_3]$ has been reacted with bpp derivatives to afford luminescent complexes of general formula $[Ru(bpp)(terpy)](PF_6)_2$.[9] However, chiral derivatives of the 1-bpp ligand have received little attention so far[12] and have never been associated to helicene units. We describe herein the synthesis of a series of bpp[*n*]helicenes ligands (*n* = 4, 4m, 5 and 6, see Scheme 1) and the following transition metal complexes: $[Re^{I}(bpp[4]helicene)(CO)_3Cl]\cdot(CH_2Cl_2)_{0.5}\cdot(H_2O)$, $[Re^{I}(bpp[5]helicene)(CO)_3Cl]$, and $[Ru^{II}(bpp[n]helicene)(terpy)](PF_6)_2$ (*n* = 4, 4m, 5 and 6). The photophysical properties of the ligands and complexes have been investigated.

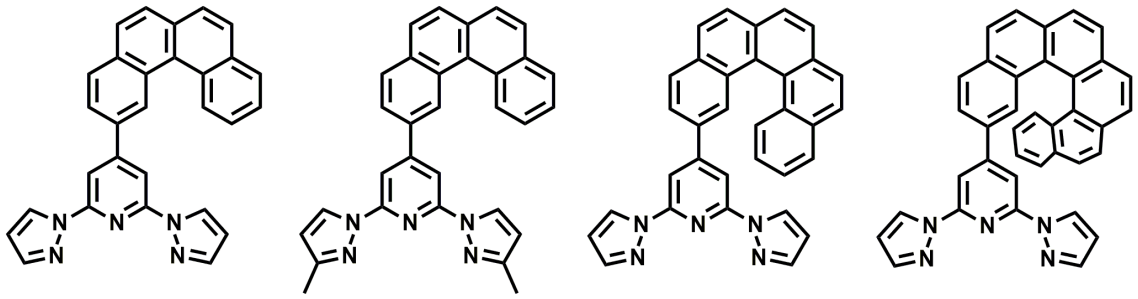

bpp[4]helicene (**4**) | me-bpp[4]helicene (**4m**) | bpp[5]helicene (**5**) | bpp[6]helicene (**6**)

Scheme 1. Bpp[*n*]helicene ligands investigated in the present study.

Results and discussion

Synthesis and crystal structures of the ligands

The synthetic procedure for the N-donor helicene-based ligands **4**, **4m**, **5** and **6** is described in Schemes 2 and 3. The preparation of bpp[*n*]helicene (*n* = 4, 5, 6) ligands has been achieved *via* a two steps procedure from racemic 2-bromo-[*n*]helicenes, synthesized according to literature reports (Scheme 2).[13] First, a Suzuki coupling between 2,6-

dichloropyridine-4-boronic acid pinacol ester and bromo[*n*]helicene afforded molecules **1**, **2** and **3** with excellent yields. These precursors were subsequently reacted with sodium pyrazolate to afford bpp[*n*]helicene ligands **4**, **5** and **6** as racemic mixtures.

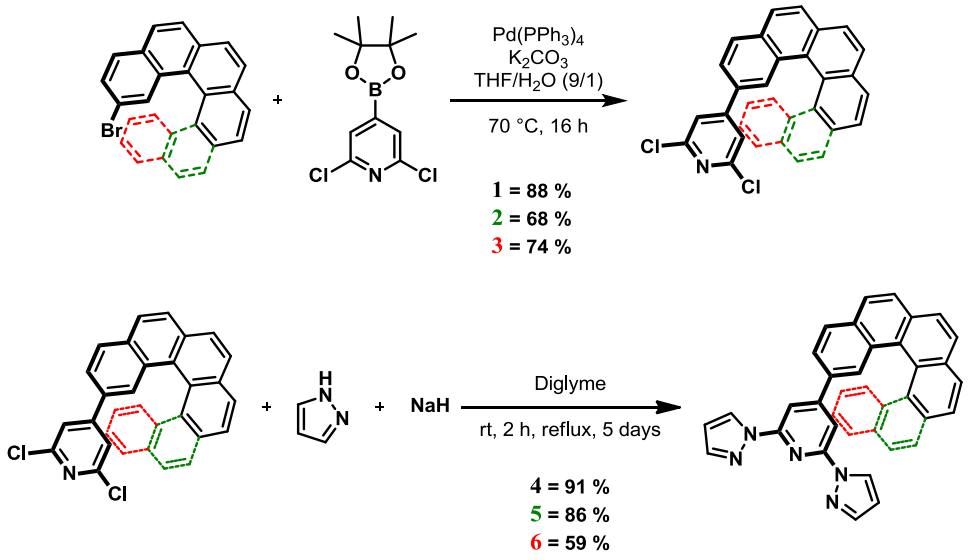

Scheme 2. Synthetic procedure for ligands **4**, **5** and **6**.

Precursor **1** has also been reacted with 3-methyl-pyrazole to prepare the ligand methyl-bpp[4]helicene **4m** (Scheme 3). This reaction provided two isomers as a consequence of the delocalization of the negative charge on both nitrogen atoms in the intermediary pyrazolate salt. As a consequence, each nitrogen atom could perform the nucleophilic attack on the dichloropyridine precursor, therefore two isomers, namely 2,6-bis(3-methylpyrazol-1-yl)pyridine-4-[4]helicene and 2-(3-methylpyrazol-1-yl)-6-(5-methylpyrazol-1-yl)pyridine-4-[4]helicene, were obtained (Scheme 3). NMR spectrum of **4m**, which as subsequently used as isomeric mixture, did not allow to conclude on the ratio between the two isomers. Note we did not observe in the reaction mixture the third possible isomer 2,6-bis(5-methylpyrazol-1-yl)pyridine-4-[4]helicene.

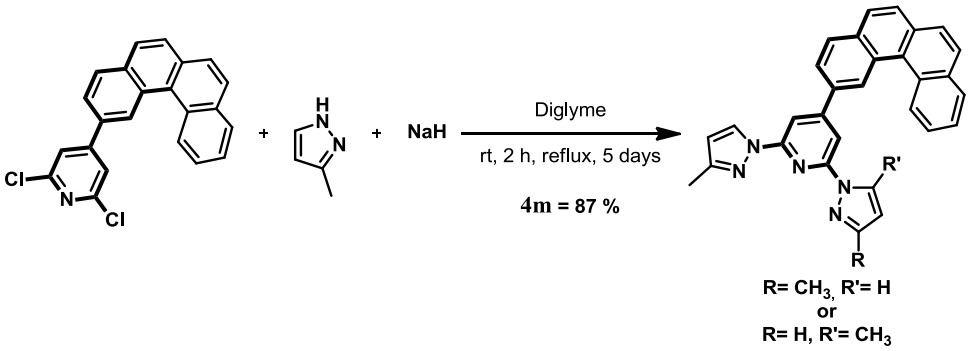

Scheme 3. Synthetic procedure for ligand **4m**.

Single crystals of **4** were obtained by slow evaporation of a chloroform solution of the ligand. The molecule crystallized in the monoclinic centrosymmetric space group $P2_1/n$. The asymmetric unit is composed of one molecule with the *P* (or *M*) conformation (Figure 1a and

Figure S1). Due to the presence of the inversion center, both *M* and *P* enantiomers are equivalently present in the crystal structure (Figure 1b). The molecule shows a dihedral angle of 33.20° between the bpp and the helicene unit, and a helical curvature of 24.54°, in line with literature values (Table S1 for bond lengths and angles).[14]

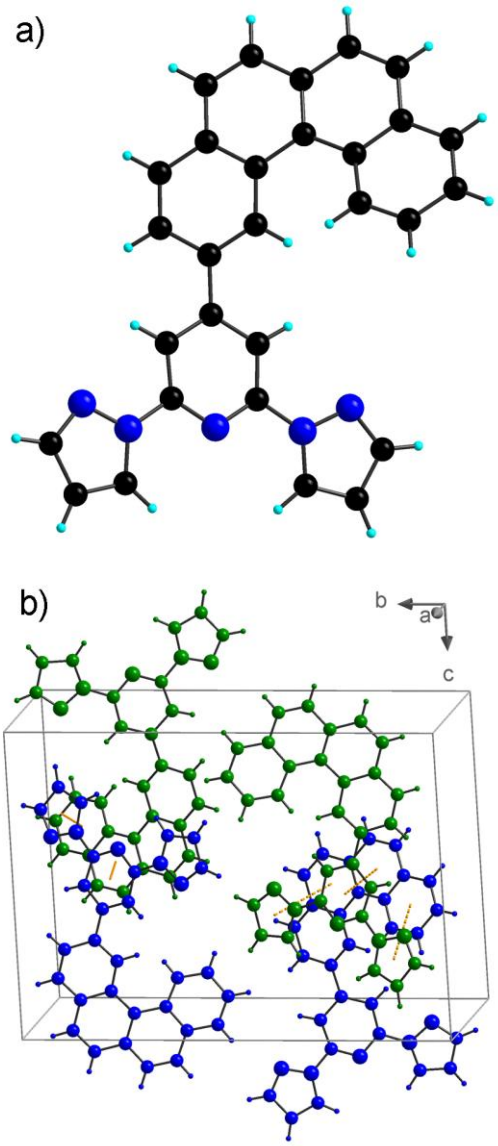

Figure 1. (a) Structure of the ligand **4**. Color code: C, black; H, cyan; N, blue. (b) Intermolecular π-π stacking in the crystal lattice. *M* and *P* enantiomers are represented in blue and green respectively.

Photophysical properties of bpp-helicenes

Figure 2 displays the absorption and room-temperature emission spectra of dichloromethane solutions of **4**, **4m**, **5** and **6**. The absorption spectra of **4** and **4m** are similar to that of a recently reported bpp ligand substituted with a methyl(phenyl)sulfane group,[11] with two charge transfer bands at around 260 and 300 nm. The spectrum of **5** slightly differs with three absorption bands at around 250, 275 and 300 nm, while **6** showed two bands shifted to lower energies (at 320 and 350 nm) and a broad absorption band between 250

and 300 nm. Therefore, emission spectra were recorded at an excitation wavelength of 300 nm for the ligands **4**, **4m** and **5**, and at 350 nm for **6**. All ligands present an emission band with two peaks. The perfect agreement between absorption and the corresponding excitation spectra (Figure S2) proves this luminescence to be intrinsic to the four compounds. According to previous studies on related bpp derivatives, this band can be attributed to ligand fluorescence.[8b] The maxima at 400 and 420 nm for both **4** and **4m** are lower in energy than in the related methylthiophenyl-bpp ligand.[11] The emission is further shifted to still lower energies in **5** (maxima at 410 and 430 nm) and in **6** (425 and 445 nm), showing that the violet fluorescence of the bpp derivative can be red shifted by increasing the number of aromatic rings in the helicene substituent. All ligands **4**, **4m**, **5** and **6** show fluorescence in the solid state upon irradiation with 365 nm UV light (Figure S3).

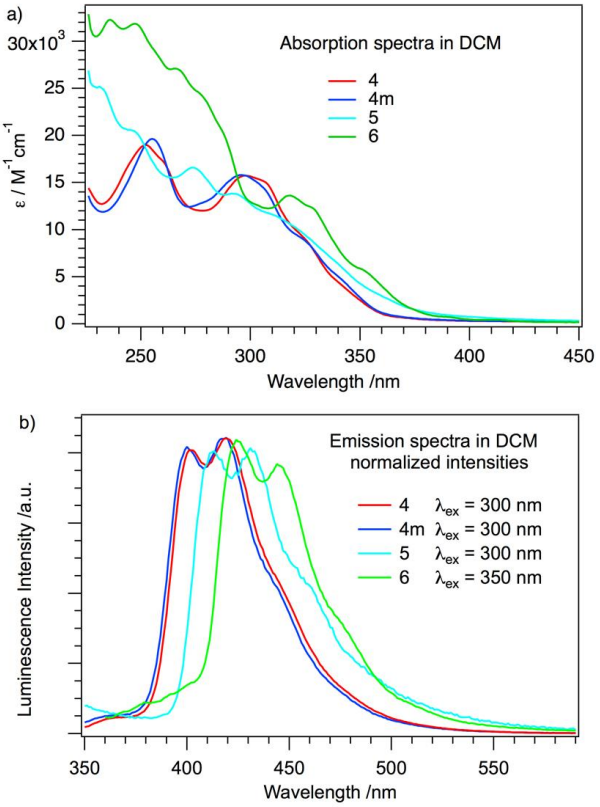

Figure 2. a) UV-Vis absorption and b) emission spectra of **4**, **4m**, **5** and **6** at room temperature in CH_2Cl_2.

Synthesis and crystal structures of the metal complexes

Metal complexes were obtained by reaction of the helicene-based ligands with the metal precursors $Re(CO)_5Cl$ and $Ru(terpy)Cl_3$) to give the compounds [Re(**4**)$(CO)_3$Cl], [Re(**5**)$(CO)_3$Cl] and [Ru(***n***)(terpy)]$(PF_6)_2$ (***n*** = **4**, **4m**, **5** and **6**). The helical bpp ligands have been attached to the [Re$(CO)_3$Cl] and [Ru(terpy)]$^{2+}$ fragments as they are well known to provide luminescent complexes. For two complexes, namely [Re(**4**)$(CO)_3$Cl] and [Ru(**4m**)(terpy)]$(PF_6)_2$, suitable single crystals for X-ray analysis have been obtained, while crystal cell determination showed that the complex [Ru(**4**)(terpy)]$(PF_6)_2$ was isostructural to the latter.

The compound [Re(**4**)$(CO)_3$Cl] crystallized in the monoclinic system, space group $P2_1/n$. The asymmetric unit is composed of one Re complex, one dichloromethane and two water solvent molecules with 0.5 occupancy (Figure 3). The Re ion is coordinated to three carbonyl ligands in a facial mode, one chloride ion and two nitrogen atoms belonging to the bpp[4]helicene ligand. As previously observed in other related Re complexes, the bpp derivative is coordinated to the metal in a bidentate mode,[8] with one pyrazolyl group remaining uncoordinated. Due to the centrosymmetric space group, both *M* and *P* enantiomeric helicenes are equivalently present in the crystal lattice. The structure can be described as bidimensional (2D) layers of *M* complexes in the [101] direction alternating along the [-101] direction with 2D layers of *P* complexes (Figure S4). Neighboring *M* and *P* complexes present intermolecular Cl···H interactions between the coordinated Cl ions and H atoms from the pyridine ring, while two consecutive *P* complexes present C–H···π interactions between helicene groups (Figure 4). The dihedral angle of 20.61° between bpp and helicene units is much lower than in the free ligand (34.24°), while the helical curvature has substantially increased (33.38° instead of 23.07° in the free ligand). This shows the easy rotation of the C–C bond between bpp and helicene parts of the ligands, which is a possible explanation for the difficulty to crystallize the bpp[*n*]helicene-based complexes.

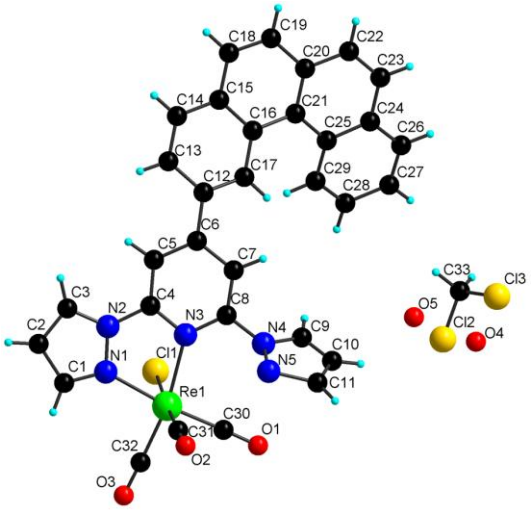

Figure 3. Structure of [Re(**4**)$(CO)_3$Cl] with atom label. Color code: C, black; H, cyan; O, red; N, blue; Cl, yellow; Re, light green.

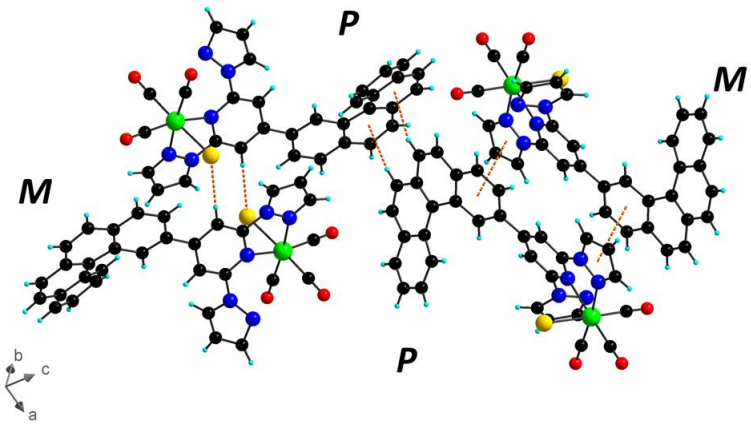

Figure 4. Illustration of the intermolecular interactions (orange dashed lines) between the complexes in [Re(**4**)$(CO)_3$Cl]. Solvent molecules are omitted for clarity. Color code: C, black; H, cyan; O, red; N, blue; Cl, yellow; Re, light green.

Compound [Ru(**4m**)(terpy)]$(PF_6)_2$ crystallized in the triclinic space group *P*-1. The asymmetric unit is composed of one Ru complex and two PF_6^- counterions (Figure 5). Structural disorder is observed for one of the two PF_6^- counterions. The Ru center is coordinated to six nitrogen atoms belonging to one terpyridine and one helicene based ligand. Ru–N bond lengths are in the range 1.975(4)–2.081(4) Å, and the octahedral environment of the Ru center is strongly distorted due to the small bite angles of the two ligands (155.78(16)° for the bpp derivative, 158.45(16)° for the terpy), as previously observed in related bpp and terpy-based Ru complexes.[9,15] Due to the inversion center, the compound crystallized as a racemic mixture, therefore both *M* and *P* enantiomers are equivalently present in the crystal structure (Figure 6). In contrast to [Re(**4**)$(CO)_3$Cl], the dihedral angle of 35.70° between bpp and helicene units in [Ru(**4m**)(terpy)]$(PF_6)_2$ is similar to that observed in the free ligand (34.24°), while the helical curvature slightly increased (29.02° instead of 23.07° in the free ligand). One of the methyl groups is disordered over positions 3 and 5 of one pyrazole ring. This observation confirmed that during the synthesis of **4m** both isomers, respectively named 2,6-bis(3-methylpyrazol-1-yl)pyridine-4-[4]helicene and 2-(3-methylpyrazol-1-yl)-6-(5-methylpyrazol-1-yl)pyridine-4-[4]helicene, were obtained (Scheme 3).

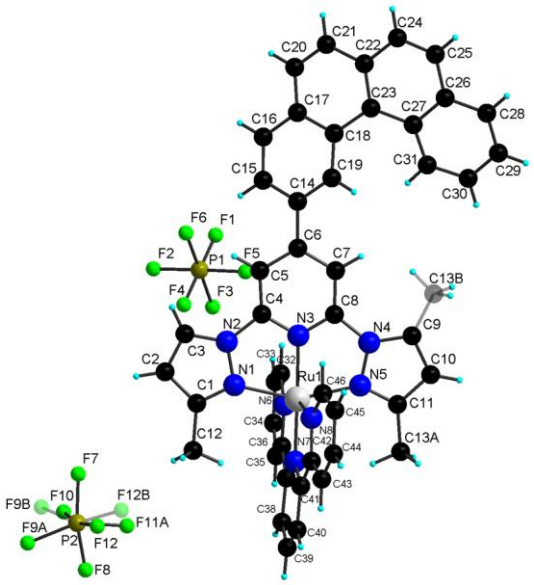

Figure 5. Structure of [Ru(**4m**)(terpy)]$(PF_6)_2$ with atom label. Color code: C, black; H, cyan; N, blue; P, olive; F, light green; Ru, grey.

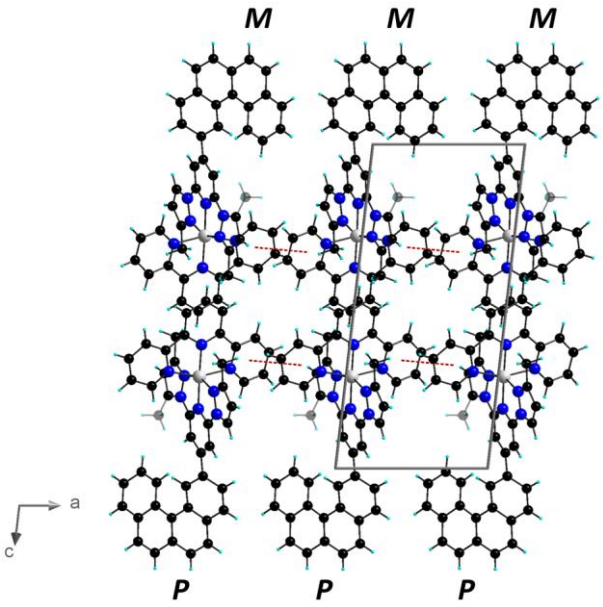

Figure 6. Crystal packing in the *ac* plane with intermolecular *π-π* stacking (red dashed lines) for [Ru(**4m**)(terpy)]$(PF_6)_2$. PF_6^- anions are omitted for clarity. Color code: C, black; H, cyan; N, blue; Ru, grey.

Photophysical Properties of the Re and Ru complexes

Figure 7 shows the absorption spectrum at room temperature and the emission spectrum at 77 K of [Re(**5**)$(CO)_3$Cl] in DCM. According to the absorption spectrum of the related complex [Re(L)$(CO)_3$Br], where L is a thiophene-substituted bpp ligand,[8b] the low-energy band at around 380 nm can be attributed to a spin-allowed metal-to-ligand charge transfer (^{1}MLCT) d → π* transition, while the higher energy bands are similar to that of the free ligand **5**. At 77 K, the complex shows a very strong luminescence, with two intense emission peaks at 540 nm and 580 nm. In the family of tricarbonyl diimine Re(I) complexes, the emission in the 500–600 nm region is usually characteristic of ^{3}MLCT phosphorescence.[16] However, by varying the nature of the ligand, this emission has in some cases been attributed to ligand-localized π-π* phosphorescence, due to the proximity of the lowest MLCT and π-π* triplet states.[17] This could also be the case in the present compound due to the extended π-system of the ligand.

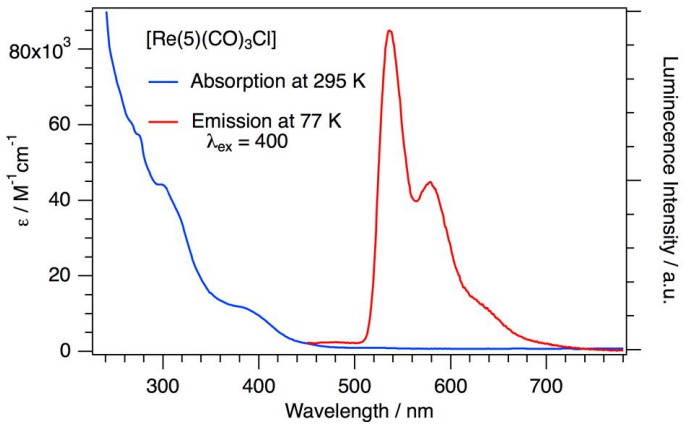

Figure 7. Absorption (blue) and emission (red) spectrum upon excitation at λ_{exc} = 400 nm of [Re(**5**)$(CO)_3$Cl] in CH_2Cl_2.

Figure 8 shows the absorption and emission spectra of the four complexes [Ru(**4**)(terpy)]$(PF_6)_2$, [Ru(**4m**)(terpy)]$(PF_6)_2$, [Ru(**5**)(terpy)]$(PF_6)_2$ and [Ru(**6**)(terpy)]$(PF_6)_2$ in acetonitrile solutions. All complexes showed a similar behavior, with a low-energy absorption band at around 450 nm corresponding to the spin-allowed ^{1}MLCT band from the metal to the terpyridine unit, and two intense bands at higher energies (at around 270 and 310 nm) corresponding to the π-π* absorptions. Luminescence spectra in frozen solutions at 77 K showed moderately intense emission bands above 600 nm. According to previous studies on bpp-based Ru(II) complexes, the emission was attributed to the radiative depopulation of terpyridine-based ^{3}MLCT states, since the weak ligand field of the bpp unit favors a rapid non-radiative decay through metal-centered (^{3}MC) states.[9]

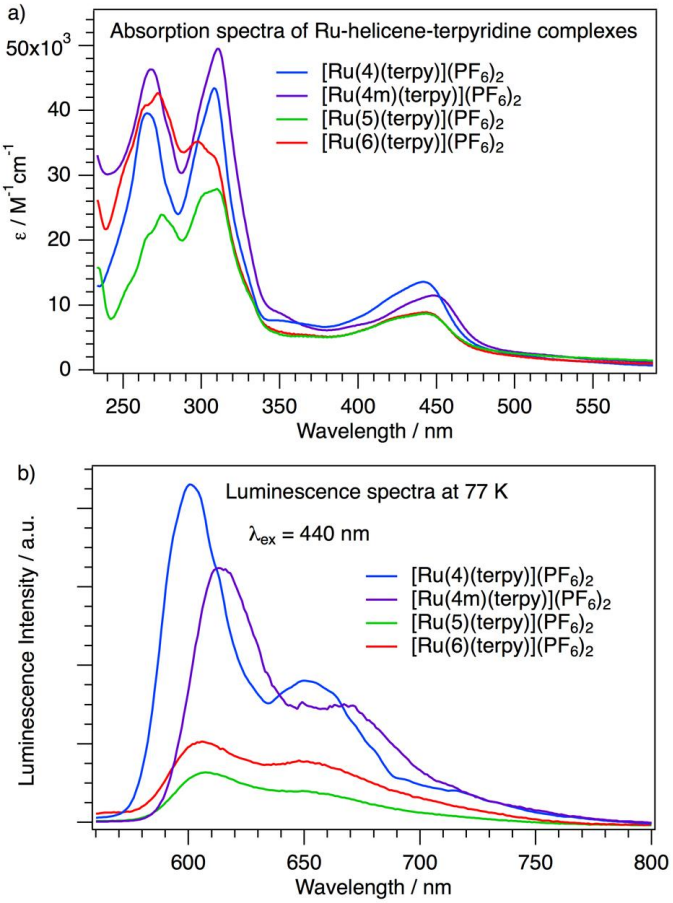

Figure 8. a) Absorption and b) emission spectra upon excitation at λ_{exc} = 440 nm of the four Ru(II) complexes in CH_3CN. Absorption spectra were recorded at room temperature and emission spectra at 77 K.

Conclusions

We have prepared helicenic ligands of the N-donating 1-bpp molecule. This series of ligands exhibit fluorescence in both the solid state and in dichloromethane solution. The new tridentate helical fluorophores have been used to prepare the Re(I) and Ru(II) complexes formulated as [Re^I(***n***)$(CO)_3Cl$] (***n*** = **4** and **5**) and [Ru^{II}(***n***)(terpy)]$(PF_6)_2$ (***n*** = **4**, **4m**, **5** and **6**). Crystal structures of [Re^I(**4**)$(CO)_3Cl$]·$(CH_2Cl_2)_{0.5}(H_2O)$ and [Ru^{II}(**4m**)(terpy)]$(PF_6)_2$ show racemic mixtures of *M* and *P* enantiomers. The tricarbonyl diimine Re(I) complex shows a very strong

emission band between 540 and 580 nm at 77 K which could arise from ligand-localized π-π* phosphorescence, while the series of Ru(II) complexes show emission bands above 600 nm, attributed to the terpyridine-based ^{3}MLCT state. These results open two possible directions of investigation. As mentioned in the Introduction bpp ligands often afford iron(II) complexes with spin crossover (SCO) properties. It would be therefore interesting to investigate the potential of the herein reported helicenic bpp's in such SCO active complexes. Secondly, the preparation of enantiomerically pure bpp-[6]helicenes, which should be conformationally stable, holds much promise in order to obtain luminescent chiral complexes possibly showing strong CPL activity.[1,3]

Experimental Section

General comments. 2-bromobenzo[c]phenanthrene,[13a] 2-bromodibenzo[c,g]phenanthrene,[13b] 2-bromohexahelicene[13c] and [Ru(terpy)Cl_3][18] were prepared according to literature methods. All other materials and solvents were commercially available and used without further purification. Infrared (IR) spectra were recorded in the solid state using a Bruker Vertex 70 spectrometer with Platinum ATR in the 400-4000 cm^{-1} range. Elemental analyses were recorded using a Flash 2000 Fisher Scientific Thermo Electron analyzer. ^{1}H and ^{13}C NMR spectra were recorded with a Bruker AVANCE III 300 (1H, 300 MHz and 13C, 75 MHz). Chemical shifts are given in ppm relative to tetramethylsilane TMS and coupling constants *J* in Hz. Residual non-deuterated solvent was used as an internal standard. A Bruker Esquire 3000 plus spectrometer was used for electrospray ionization mass spectrometry (ESI-MS).

Synthesis of 4-(benzo[c]phenanthren-2-yl)-2,6-dichloropyridine (1). In a Schlenk tube under argon were dissolved 2-bromobenzo[*c*]phenanthrene (168 mg, 0.55 mmol), $Pd(PPh_3)_4$ (21 mg, 18 µmol) and 2,6-dichloropyridinyl-4-boronic acid pinacol ester (100 mg, 0.37 mmol) in 9.5 mL of THF. After degassing with argon for 10 min, a degassed solution of potassium carbonate (126 mg, 0.91 mmol) in H_2O (1.5 mL) was added. The mixture was stirred at 70 °C for 16 h, then cooled to room temperature and then CH_2Cl_2 (20 mL) was added. The organic layer was washed 3 times with water, 3 times with brine and then dried over $MgSO_4$. The crude product was concentrated under vacuum and purified by column chromatography on silica gel (9/1 petroleum ether/EtOAc as eluent) to afford **1** as a white powder (120 mg, 88 % yield). ^{1}H NMR (300 MHz, Chloroform-*d*): δ 9.33 (d, *J* = 1.4 Hz, 1H), 9.03 (d, *J* = 8.4 Hz, 1H), 8.15 (d, *J* = 8.4 Hz, 1H), 8.08 (dd, *J* = 8.0, 1.3 Hz, 1H), 7.98 (d, *J* = 8.5 Hz, 1H), 7.94 (d, *J* = 1.5 Hz, 2H), 7.87 (d, *J* = 8.6 Hz, 1H), 7.82 (dd, *J* = 8.3, 1.8 Hz, 1H), 7.77 (ddd, *J* = 8.5, 6.9, 1.5 Hz, 1H), 7.70 (ddd, *J* = 7.9, 6.9, 1.1 Hz, 1H), 7.64 (s, 2H). ^{13}C NMR (76 MHz, Chloroform-*d*): δ 154.5, 151.2, 134.2, 133.7, 133.2, 131.5, 130.5, 130.0, 129.8, 129.7, 128.9, 128.8, 128.6, 128.3, 127.5, 127.4, 127.3, 127.1, 126.9, 126.4, 124.1. FAB+ m/z = 373.0424.

Synthesis of 2,6-dichloro-4-(dibenzo[c,g]phenanthren-9-yl)pyridine (2). Compound **2** was synthesized in a similar manner to **1** but using 2-bromodibenzo[*c*,*g*]phenanthrene (215 mg, 0.60 mmol) instead of 2-bromobenzo[*c*]phenanthrene, $Pd(PPh_3)_4$ (23.2 mg, 20 µmol), 2,6-dichloropyridinyl-4-boronic acid pinacol ester (110 mg, 0.40 mmol) and potassium carbonate (138 mg, 1.0 mmol). After purification, compound **2** was obtained as a white solid (115 mg, 68 % yield). ^{1}H NMR (300 MHz, Chloroform-*d*): δ 8.84 (s, 1H), 8.59 (d, *J* = 8.4 Hz, 1H), 8.05

(dd, *J* = 7.9, 5.9 Hz, 2H), 7.94 (m, 6H), 7.71 (dd, *J* = 8.4, 1.9 Hz, 1H), 7.63 (ddd, *J* = 8.1, 6.9, 1.2 Hz, 1H), 7.37 (ddd, *J* = 8.4, 6.9, 1.4 Hz, 1H), 7.31 (s, 2H). ^{13}C NMR (76 MHz, Chloroform-*d*): δ 153.8, 151.0, 135.6, 135.0, 133.4, 133.2, 132.8, 132.7, 131.3, 130.8, 130.7, 129.8, 129.4, 128.7, 128.5, 128.3, 128.1, 127.5, 127.2, 127.0, 126.9, 126.7, 124.9, 124.4, 120.9. FAB+ m/z = 423.0582.

Synthesis of 2,6-dichloro-4-(hexahelicen-11-yl)pyridine (3). Compound **3** was synthesized in a similar manner to **1** but using 2-bromohexahelicene (245 mg, 0.60 mmol) instead of 2-bromobenzo[*c*]phenanthrene, $Pd(PPh_3)_4$ (23.2 mg, 20 µmol), 2,6-dichloropyridinyl-4-boronic acid pinacol ester (110 mg, 0.40 mmol) and potassium carbonate (138 mg, 1.0 mmol). After purification, compound **3** was obtained as a white solid (140 mg, 74 % yield). ^{1}H NMR (300 MHz, Chloroform-*d*): δ 8.11 – 7.99 (m, 8H), 7.98 (d, *J* = 1.8 Hz, 1H), 7.97 – 7.91 (m, 3H), 7.67 (d, *J* = 8.7 Hz, 1H), 7.40 (dd, *J* = 8.3, 1.9 Hz, 1H), 6.74 (ddd, *J* = 8.5, 6.9, 1.4 Hz, 1H), 6.61 (s, 2H). ^{13}C NMR (76 MHz, Chloroform-*d*): δ 153.65, 150.56, 133.57, 132.61, 132.43, 132.15, 131.94, 129.87, 129.64, 129.06, 128.25, 128.20, 128.13, 127.90, 127.85, 127.68, 127.64, 127.55, 127.44, 127.03, 126.47, 125.22, 123.98, 123.74, 120.75. MS (EI) m/z = 473.0733.

Synthesis of 2,6-bis(pyrazol-1-yl)pyridine-4-[4]helicene (bpp[4]helicene, 4). Under nitrogen atmosphere, pyrazole (121 mg, 1.78 mmol) was dissolved in diethylene glycol dimethyl ether (10 mL) and NaH (60 %w, 71 mg, 1.78 mmol) was slowly added. After 2h of stirring at room temperature, **1** (230 mg, 0.61 mmol) was added and the resulting mixture was heated under reflux for 5 days. Then the solvent was evaporated and **4** was precipitated by addition of water (20 mL). The white powder was filtrated and dried under vacuum (254 mg, 0.58 mmol, 91 % yield). White crystals suitable for X-ray diffraction were obtained by recrystallization of the powder in chloroform. ^{1}H NMR (300 MHz, Chloroform-*d*): δ 9.52 (s, 1H), 9.15 (d, *J* = 8.7 Hz, 1H), 8.65 (d, *J* = 2.4 Hz, 2H), 8.29 (s, 2H), 8.13 (d, *J* = 8.4 Hz, 1H), 8.05 (d, *J* = 6.9 Hz, 1H), 8.03 (dd, *J* = 8.1, 1.8 Hz, 1H), 7.97 – 7.83 (m, 5H), 7.81 (d, *J* = 0.9 Hz, 2H), 7.76 (ddd, *J* = 8.4, 7.2 Hz, 1.2 Hz, 1H), 7.65 (ddd, *J* = 8.1, 6.9 Hz, 0.9 Hz, 1H), 6.54 (dd, *J* = 2.4, 2.1 Hz, 2H). ^{13}C NMR (76 MHz, Chloroform-*d*): δ 154.8, 150.8, 142.4, 135.2, 134.0, 133.6, 129.4, 128.7, 128.0, 127.8, 127.3, 127.1, 127.0, 126.8, 126.7, 126.3, 124.7, 108.0, 107.8. MS (EI) m/z = 437.1639 (calcd: 437.1640).

Synthesis of 2,6-bis(3-methylpyrazol-1-yl)pyridine-4-[4]helicene (me-bpp[4]helicene, 4m). 4m was synthesized in a similar manner to **4** but using 3-methylpyrazole (68 µL, 0.84 mmol) instead of pyrazole, NaH (60 %w, 34 mg, 0.84 mmol) and **1** (108 mg, 0.29 mmol). A white powder was obtained (117 mg, 0.25 mmol, 87 % yield). ^{1}H NMR (300 MHz, Chloroform-*d*): δ 9.52 (s, 1H), 9.19 (d, *J* = 8.4 Hz, 1H), 8.52 (d, *J* = 2.1 Hz, 2H), 8.19 (s, 2H), 8.14 (d, *J* = 8.7 Hz, 1H), 8.05 (d, *J* = 7.5 Hz, 2H), 7.97 – 7.84 (m, 5H), 7.76 (t, *J* = 7.5 Hz, 1H), 7.66 (t, *J* = 6.3 Hz, 1H), 6.31 (d, *J* = 2.1 Hz, 2H), 2.43 (s, 6H). ^{13}C NMR (76 MHz, Chloroform-*d*): δ 152.0, 150.7, 133.9, 133.6, 131.4, 130.2, 129.2, 128.7, 127.9, 127.0, 126.7, 126.2, 124.8, 108.1, 106.9. MS (EI) m/z = 465.1946 (calcd: 465.1953).

Synthesis of 2,6-bis(pyrazol-1-yl)pyridine-4-[5]helicene (bpp[5]helicene, 5). 5 was synthesized in a similar manner to **4** but using pyrazole (52 mg, 0.76 mmol), NaH (60 % w, 31 mg, 0.76 mmol) and **2** (112 mg, 0.26 mmol) instead of **1**. A white powder was obtained (109 mg, 0.22 mmol, 86 % yield). ^{1}H NMR (300 MHz, Chloroform-*d*): δ 9.01 (s, 1H), 8.70 (d, *J* = 8.4

Hz, 1H), 8.55 (d, *J* = 2.4 Hz, 2H), 8.09 (d, *J* = 8.4 Hz, 1H), 8.02 (d, *J* = 7.2 Hz, 1H), 7.92 (m, 8H), 7.79 (d, *J* = 0.9 Hz, 2H), 7.68 (ddd, *J* = 8.1, 6.9, 1.2 Hz, 1H), 7.47 (ddd, *J* = 8.4, 6.9, 1.4 Hz, 1H), 6.50 (dd, *J* = 2.7, 2.4 Hz, 2H). ^{13}C NMR (76 MHz, Chloroform-*d*): δ 154.4, 150.5, 142.1, 133.6, 133.1, 132.9, 132.6, 132.4, 130.9, 128.9, 128.3, 128.0, 128.0, 127.9, 127.8, 127.7, 127.3, 127.2, 127.1, 127.0, 126.9, 126.3, 125.2, 125.1, 107.9, 107.8. MS (EI) m/z = 487.1789 (calcd: 487.1797).

Synthesis of 2,6-bis(pyrazol-1-yl)pyridine-4-[6]helicene (bpp[6]helicene, 6). **6** was synthesized in a similar manner to **4** but using pyrazole (59 mg, 0.86 mmol), NaH (60%w, 35 mg, 0.86 mmol) and **3** (140 mg, 0.30 mmol) instead of **1**. A white powder was obtained (95 mg, 0.18 mmol, 59% yield). ^{1}H NMR (300 MHz, Chloroform-*d*): δ 8.52 (dd, J = 2.7, 0.9 Hz, 1H), 8.09 – 7.89 (m, 11H), 7.87 (dt, *J* = 1.5, 0.6 Hz, 2H), 7.74 (d, *J* = 0.9 Hz, 1H), 7.66 (m, 2H), 7.55 (d, *J* = 8.7 Hz, 1H), 7.32 (s, 1H), 7.20 (ddd, *J* = 7.2, 6.9, 1,2 Hz, 1H), 6.73 (m, 1H), 6.51 (dd, *J* = 2.7, 2.4 Hz, 1H). ^{13}C NMR (76 MHz, Chloroform-*d*): δ 154.2, 150.2, 141.9, 133.1, 132.3, 131.6, 130.6, 130.2, 129.5, 128.9, 128.6, 128.1, 127.8, 127.8, 127.7, 127.6, 127.5, 127.4, 127.3, 127.2, 127.1, 127.0, 126.9, 126.8, 126.2, 126.0, 125.7, 124.7, 124.7, 124.6, 119.1, 107.8, 107.5. MS (EI) m/z = 537.1943 (calcd: 537.1953).

Synthesis of the complex [Re(4)(CO)$_3$Cl]·(CH$_2$Cl$_2$)$_{0.5}$(H$_2$O). To a solution of **4** (22 mg, 0.05 mmol) in toluene (10 mL) was added ReCl(CO)$_5$ (18 mg, 0.05 mmol). The solution was stirred under reflux for 6h, and the solvent was removed by vacuum. The obtained brown powder (20 mg, 50 % yield) was recrystallized in dichloromethane to afford yellow crystals after slow evaporation of the solvent. ESI-MS (positive mode): *m/z* = 708.09 (calcd *m/z* of 708.10 for [Re(**4**)(CO)$_3$]$^-$).

Synthesis of the complex [Re(5)(CO)$_3$Cl]. [Re(5)(CO)$_3$Cl] was synthesized in a similar manner to [Re(**4**)(CO)$_3$Cl] but using **5** (24 mg, 0.05 mmol) instead of **4**. Recrystallization of the residue in dichloromethane afforded [Re(**5**)(CO)$_3$Cl] as a yellow powder (20 mg, 50 % yield). Thermogravimetric analysis (TGA) showed no weight loss before 200°C, confirming the absence of solvent molecules (Figure S8 in the SI). MALDI: *m/z* = 729.9 (calcd *m/z* of 730.13 for [Re(**5**)(CO)$_2$]$^+$), *m/z* = 758.0 (calcd *m/z* of 758.12 for [Re(**5**)(CO)$_3$]$^+$), *m/z* = 765.0 (calcd *m/z* of 765.09 for [Re(**5**)(CO)$_2$Cl]).

Synthesis of the complex [Ru(4)(terpy)](PF$_6$)$_2$. To a suspension of **4** (11 mg, 0.025 mmol) in absolute ethanol (10 mL) was added [Ru(terpy)Cl$_3$] (11 mg, 0.025 mmol) and AgNO$_3$ (13 mg, 0.075 mmol). The suspension was stirred overnight under reflux. The resulting orange mixture was filtered to remove AgCl, and a solution of NH$_4$PF$_6$ (82 mg, 0.5 mmol) in MeOH (5 mL) was added to the filtrate. The brown precipitate was filtered, washed with EtOH and dried under vacuum (6 mg, 23% yield). Red prismatic crystals were obtained by slow diffusion of diethylether in an acetonitrile solution of the complex. ESI-MS (positive mode): *m/z* = 386.01 (calcd *m/z* of 386.08 for [Ru(**4**)(terpy)]$^{2+}$), 917.04 (calcd *m/z* of 917.13 for {[Ru(**4**)(terpy)](PF$_6$)}$^+$). Anal. calc. for C$_{44}$H$_{30}$N$_8$F$_{12}$P$_2$Ru: C, 49.77; H, 2.85; N, 10.55%. Found: C, 48.63; H, 2.84; N, 10.36%.

Synthesis of the complex [Ru(4m)(terpy)](PF$_6$)$_2$. [Ru(4m)(terpy)](PF$_6$)$_2$ was synthesized in a similar manner to [Ru(**4**)(terpy)](PF$_6$)$_2$ but using **4m** (47 mg, 0.10 mmol) instead of **4**,

[Ru(terpy)Cl_3] (44 mg, 0.10 mmol), $AgNO_3$ (51 mg, 0.30 mmol) and NH_4PF_6 (326 mg, 2.00 mmol) (26 mg, 25 % yield). Red prismatic crystals were obtained by slow diffusion of diethylether in an acetonitrile solution of the complex. ESI-MS (positive mode): *m/z* = 399.87 (calcd *m/z* of 400.10 for [Ru(**4m**)(terpy)]$^{2+}$), 945.03 (calcd *m/z* of 945.16 for {[Ru(**4m**)(terpy)](PF_6)}$^+$). Anal. calc. for $C_{46}H_{34}N_8F_{12}P_2Ru$: C, 50.70; H, 3.14; N, 10.28%. Found: C, 49.95; H, 3.03; N, 10.09%

Synthesis of the complex [Ru(5)(terpy)]$(PF_6)_2$. [Ru(5)(terpy)]$(PF_6)_2$ was synthesized in a similar manner to [Ru(**4**)(terpy)]$(PF_6)_2$ but using **5** (7.0 mg, 0.014 mmol) instead of **4**, [Ru(terpy)Cl_3] (6.2 mg, 0.014 mmol), $AgNO_3$ (7.1 mg, 0.042 mmol) and NH_4PF_6 (46 mg, 0.28 mmol) (4.1 mg, 26 % yield). A red powder was obtained by slow diffusion of diethylether in an acetonitrile solution of the complex. ESI-MS (positive mode): *m/z* = 411.00 (calcd *m/z* of 411.09 for [Ru(**5**)(terpy)]$^{2+}$), 967.01 (calcd *m/z* of 967.14 for {[Ru(**5**)(terpy)](PF_6)}$^+$).

Synthesis of the complex [Ru(6)(terpy)]$(PF_6)_2$. [Ru(6)(terpy)]$(PF_6)_2$ was synthesized in a similar manner to [Ru(**4**)(terpy)]$(PF_6)_2$ but using **6** (10.8 mg, 0.02 mmol) instead of **4**, [Ru(terpy)Cl_3] (8.8 mg, 0.02 mmol), $AgNO_3$ (10.2 mg, 0.06 mmol) and NH_4PF_6 (65 mg, 0.40 mmol) (9.5 mg, 41 % yield). A red powder was obtained by slow diffusion of diethylether in an acetonitrile solution of the complex. ESI-MS (positive mode): *m/z* = 435.97 (calcd *m/z* of 436.10 for [Ru(**6**)(terpy)]$^{2+}$), 1017.02 (calcd *m/z* of 1017.16 for {[Ru(**6**)(terpy)](PF_6)}$^+$).

Structural Characterization

Single crystals of the compounds were mounted on glass fiber loops using a viscous hydrocarbon oil to coat the crystal and then transferred directly to the cold nitrogen stream for data collection. Data collections were performed at 150 K (for compounds **4** and [Re(**4**)$(CO)_3Cl$]) or at 296 K (for compounds [Ru(**4**)(terpy)]$(PF_6)_2$ and [Ru(**4m**)(terpy)]$(PF_6)_2$) on an Agilent Supernova with Cu$K\alpha$ (λ = 1.54184 Å). The structures were solved by direct methods with the SIR97 program and refined against all F^2 values with the SHELXL-97 program[19] using the WinGX graphical user interface.[20] All non-hydrogen atoms were refined anisotropically except as noted. Hydrogen atoms were placed in calculated positions and refined isotropically with a riding model, except hydrogen atoms belonging to the $H_9O_4^+$ cationic entities. The program SQUEEZE from PLATON was used to calculate the potential solvent accessible void volume and the nature of the disordered solvent molecules. A summary of the crystallographic data and the structure refinement is given in Table 1. CCDC 1919203 (**4**), CCDC 1919204 ([Re(**4**)$(CO)_3Cl$]) and CCDC 1919205 ([Ru(**4m**)(terpy)]$(PF_6)_2$) contain the supplementary crystallographic data for this paper. This data can be obtained free of charge from The Cambridge Crystallographic Data Centre via www.ccdc.cam.ac.uk/data_request/cif.

Table 1. Crystallographic data for compounds **4**, [Re(**4**)$(CO)_3Cl$], [Ru(**4**)(terpy)]$(PF_6)_2$ and [Ru(**4m**)(terpy)]$(PF_6)_2$.

	4	**[Re(4)$(CO)_3Cl$]**	**[Ru(4)(terpy)]$(PF_6)_2$**	**[Ru(4m)(terpy)]$(PF_6)_2$**
Empirical formula	$C_{29}H_{19}N_5$	$C_{32.5}H_{22}N_5O_4Cl_2Re$	$C_{44}H_{30}F_{12}N_8P_2Ru$	$C_{46}H_{34}F_{12}N_8P_2Ru$
Fw	437.49	803.65	1061.77	1089.82
Crystal color	Yellow	Yellow	Red	Red

Crystal size (mm^3)	0.5*0.45*0.35	0.4*0.04*0.02	0.04*0.03*0.02	0.03*0.03*0.01
Temperature (K)	150	150	296	296
Wavelength (Å)	1.54184	1.54184	1.54184	1.54184
Crystal system, Z	Monoclinic, 4	Monoclinic, 4	Triclinic, 2	Triclinic, 2
Space group	$P2_1/n$	$P2_1/n$	P-1	P-1
a (Å)	7.48210(10)	15.0302(4)	9.172(4)	9.1242(4)
b (Å)	19.7127(3)	7.5372(2)	12.477(3)	12.5519(7)
c (Å)	14.2615(3)	27.6224(7)	20.094(5)	20.1006(10)
α (°)	90	90	102.70(3)	103.381(5)
β (°)	90.714(2)	93.793(3)	95.31(3)	96.362(4)
γ (°)	90	90	90.12(2)	90.171(4)
V (Å³)	2103.30(6)	3122.37(14)	2233.1(12)	2224.78(19)
ρ_{calc} ($g.cm^{-3}$)	1.382	1.710		1.627
μ(CuKα) (mm^{-1})	0.663	9.569		4.385
θ range (°)	3.826–73.352	3.207–73.452		3.621–73.458
Data collected	7738	12481		16584
Data unique	3964	6069		8605
Data observed	3601	5526		6928
R(int)	0.0175	0.0219		0.0504
Nb of parameters / restraints	308/0	394/1		649/0
$R1(F)$,[a] $I > 2\sigma(I)$	0.0351	0.0523		0.0575
$wR2(F^2)$,[b] all data	0.0957	0.1564		0.1605
$S(F^2)$,[c] all data	1.043	1.118		1.038

[a] $R1(F) = \Sigma\|F_0|-|F_C\|/\Sigma|F_0|$; [b] $wR2(F^2) = [\Sigma w(F_0^2-F_C^2)^2/\Sigma wF_0^4]^{1/2}$; [c] $S(F^2) = [\Sigma w(F_0^2-F_C^2)^2/(n+r-p)]^{1/2}$.

Photophysical measurements

Absorption spectra of DCM solutions of the respective free ligands and rhenium complex and of acetonitrile solutions of the ruthenium complexes at room temperature were recorded on a Cary 5000 spectrometer (Agilent). Luminescence and excitation spectra of the free ligands at room temperature and of the complexes in frozen solutions in the same solvents at 77 K were recorded on a Fluorolog 3 (Horiba-Jobin Yvon). These were corrected for the spectral response of the spectrometer.

Acknowledgements

The authors thank the CNRS, the University of Angers and the RFI Regional project LUMOMAT (grant to A.A., project ASCO MMM). Ingrid Freuze and Sonia Jerjir (University of Angers) are gratefully acknowledged for MS characterization of the complexes.

Notes and references

[1] F. Pop, N. Zigon, N. Avarvari, *Chem. Rev.* **2019**, *119*, 8435–8478.

[2] a) M. Gingras, *Chem. Soc. Rev.* **2013**, *42*, 1051–1095; b) J. Bosson, J. Gouin, J. Lacour, *Chem. Soc. Rev.* **2014**, *43*, 2824–2840; c) Y. Shen, C.-F. Chen, *Chem. Rev.* **2012**, *112*, 1463–1535.

[3] a) N. Saleh, C. Shen, J. Crassous, *Chem. Sci.* **2014**, *5*, 3680–3694; b) E. Anger, M. Srebro, N. Vanthuyne, L. Toupet, S. Rigaut, C. Roussel, J. Autschbach, J. Crassous, R. Réau, *J. Am. Chem. Soc.* **2012**, *134*, 15628–15631; c) M. Srebro, E. Anger, B. Moore, N. Vanthuyne, C. Roussel, R. Réau, J. Autschbach, J. Crassous, *Chem. Eur. J.* **2015**, *21*, 1673–1681; d) C. Shen, G. Loas, M.

Srebro-Hooper, N. Vanthuyne, L. Toupet, O. Cador, F. Paul, J. T. López Navarrete, F. J. Ramírez, B. Nieto-Ortega, J. Casado, J. Autschbach, M. Vallet, J. Crassous, *Angew. Chem. Int. Ed.* **2016**, *128*, 8194–8198; e) T. Biet, T. Cauchy, Q. Sun, J. Ding, A. Hauser, P. Oulevey, T. Bürgi, D. Jacquemin, N. Vanthuyne, J. Crassous, N. Avarvari, *Chem. Commun.* **2017**, *53*, 9210–9213.

[4] J. Míšek, F. Teplý, I. G. Stará, M. Tichý, D. Šaman, I. Císařová, P. Vojtíšek, I. Starý, *Angew. Chem. Int. Ed.* **2008**, *47*, 3188–3191.

[5] a) N. Saleh, B. Moore, M. Srebro, N. Vanthuyne, L. Toupet, J. A. Gareth Williams, C. Roussel, K. K. Deol, G. Muller, J. Autschbach, J. Crassous, *Chem. Eur. J.* **2015**, *21*, 1673–1681; b) H. Isla, M. Srebro-Hooper, M. Jean, N. Vanthuyne, T. Roisnel, J. L. Lunkley, G. Muller, J. A. Gareth Williams, J. Autschbach, J. Crassous, *Chem. Commun.* **2016**, *52*, 5932–5935.

[6] M. A. Halcrow, *Coord. Chem. Rev.* **2005**, *249*, 2880–2908.

[7] a) M. A. Halcrow, *Coord. Chem. Rev.* **2009**, *253*, 2493–2514; b) M. A. Halcrow, *New J. Chem.* **2014**, *38*, 1868–1882; c) T. Buchen, P. Gütlich, K. H. Sugiyarto, H. A. Goodwin, *Chem. Eur. J.* **1996**, *2*, 1134–1138; d) S. Marcen, L. Lecren, L. Capes, H. A. Goodwin, J. F. Létard, *Chem. Phys. Lett.* **2002**, *358*, 87–95; e) G. Chastanet, C. A. Tovee, G. Hyett, M. A. Halcrow, J. F. Létard, *Dalton Trans.* **2012**, *41*, 4896–4902.

[8] a) B. Machura, R. Penczek, R. Kruszynski, *Polyhedron* **2007**, *26*, 2470–2476; b) L. A. Lytwak, J. M. Stanley, M. L. Mejía, B. J. Holliday, *Dalton Trans.* **2010**, *39*, 7692–7699.

[9] a) F. Schamm, R. Chandrasekar, T. A. Zevaco, M. Rudolph, H. Görls, W. Poppitz, M. Ruben, *Eur. J. Inorg. Chem.* **2009**, 53–61; b) X. J. Zhu, B. J. Holliday, *Macromol. Rapid Commun.* **2010**, *31*, 904–909.

[10] S. Basak, P. Hui, S. Boodida, R. Chandrasekar, *J. Org. Chem.* **2012**, *77*, 3620–3626.

[11] U. Venkataramudu, C. Sahoo, S. Leelashree, M. Venkatesh, D. Ganesh, S. R. G. Naraharisetty, A. K. Chaudhary, S. Srinath, R. Chandrasekar, *J. Mater. Chem. C* **2018**, *6*, 9330–9335.

[12] a) A. A. Watson, D. A. House, P. J. Steel, *J. Org. Chem.* **1991**, *56*, 4072–4074; b) D. D. LeCloux, W. B. Tolman, *J. Am. Chem. Soc.* **1993**, *115*, 1153–1154; c) D. L. Christenson, C. J. Tokar, W. B. Tolman, *Organometallics* **1995**, *14*, 2148–2150; d) W.-H. Fung, W.-Y. Yu, C.-M. Che, *J. Org. Chem.* **1998**, *63*, 7714–7726; e) R. Kowalczyk, J. Skarzewski, *Tetrahedron* **2005**, *61*, 623–628.

[13] a) M. A. Brooks, L. T. Scott, *J. Am. Chem. Soc.* **1999**, *121*, 5444–5449; b) R. El Abed, B. Ben Hassine, J.-P. Genêt, M. Gorsane, A. Marinetti, *Eur. J. Org. Chem.* **2004**, 1517–1522; c) M. Jakubec, T. Beránek, P. Jakubík, J. Sýkora, J. Žádný, V. Církva, J. Storch, *J. Org. Chem.* **2018**, *83*, 3607–3616.

[14] T. Biet, A. Fihey, T. Cauchy, N. Vanthuyne, C. Roussel, J. Crassous, N. Avarvari, *Chem. Eur. J.* **2013**, *19*, 13160–13167.

[15] A. I. Philippopoulos, A. Terzis, C. P. Raptopoulou, V. J. Catalano, P. Falaras, *Eur. J. Inorg. Chem.* **2007**, 5633–5644.

[16] a) A. J. Amoroso, M. P. Coogan, J. E. Dunne, V. Fernández-Moreira, J. B. Hess, A. J. Hayes, D. Lloyd, C. Millet, S. J. A. Pope, C. Williams, *Chem. Commun.* **2007**, 3066–3068; b) S.-T. Lam, N. Zhu, V. W.-W. Yam, *Inorg. Chem.* **2009**, *48*, 9664–9670; c) M.-W. Louie, H.-W. Liu, M. H.-C. Lam, T.-C. Lau, K. K.-W. Lo, *Organometallics* **2009**, *28*, 4297–4307; d) M. R. Waterland, T. J. Simpson, K. C. Gordon, A. K. Burrell, *J. Chem. Soc., Dalton Trans.* **1998**, 185–192; e) Y. Wang, B. T. Hauser, M. M. Rooney, R. D. Burton, K. S. Schanze, *J. Am. Chem. Soc.* **1993**, *115*, 5675–5683.

[17] L. Sacksteder, A. P. Zipp, E. A. Brown, J. Streich, J. N. Demas, B. A. DeGraff, *Inorg. Chem.* **1990**, *29*, 4335–4340.

[18] B. P. Sullivan, J. M. Calvert, T. J. Meyer, *Inorg. Chem.* **1980**, *19*, 1404–1407.

[19] G. M. Sheldrick, *Programs for the Refinement of Crystal Structures;* University of Göttingen: Göttingen, Germany, **1996**.

[20] L. J. Farrugia, *J. Appl. Crystallogr.* **1999**, *32*, 837–838.

Table of Contents Entry

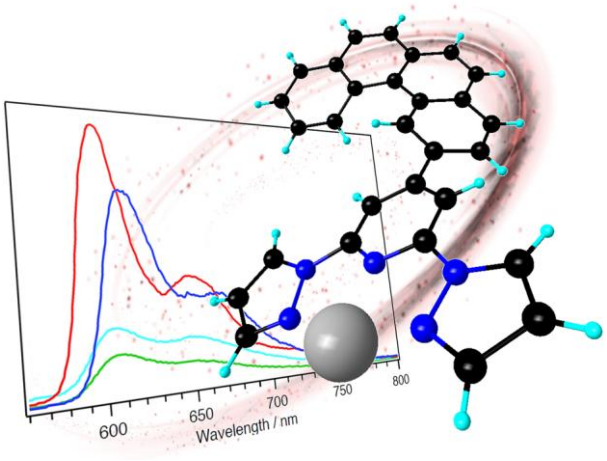

Synthesis, single crystal X-ray structures and photophysical properties of unprecedented helicene containing 2,6-bis(pyrazolyl)pyridine ligands and corresponding Re(I) and Ru(II) complexes are reported. Both the ligands and the Ru(II) complexes show fluorescence properties in the violet and blue regions respectively, while the Re(I) complex exhibits strong phosphorescence at 77 K.

Key Topic: bis(pyrazolyl)pyridine; helicene-based complexes; luminescence